show a relatively strong band at 1316 $\mathrm{cm^{-1}}$, characteristic of neutral DPP ligand. Although the signal:noise ratio is lower,[9] the spectrum obviously resembles that of the ground-state, but under the saturation conditions that prevail, the scattering cannot arise from the ground state and must therefore be attributed to vibrational modes of the neutral ligand, in the MLCT excited state of the complex. The resonance enhancement here is principally ascribed to a LMCT transition (from neutral DPP ligand to the formal[4a] $\mathrm{Cu^{II}}$ center), which in this bis(ligand) complex is the probable major source of the excited-state absorption in the 360-nm region.

By selective excitation in different absorption bands of the MLCT excited state of $[\mathrm{Cu(DPP)_2}]^+$ we have therefore been able to observe resonantly enhanced Raman features characteristic of either the neutral DPP ligand or the radical anion. This provides convincing evidence for a localized formulation of the excited state: $[\mathrm{Cu^{II}(L)(L^{\bullet -})}]^+$, on the 10-ns timescale of the present experiments. The results, which are the first of this type reported for the excited states of $\mathrm{d^{10}}$ transition-metal complexes, are a further example of the potential of resonance Raman spectroscopy for the investigation of charge-transfer excited states. Furthermore, the ability of the technique, demonstrated in the present work and elsewhere,[1,2,10] to selectively monitor both "neutral" and electron-rich or electron-deficient regions of molecules suggests its wider application as a structural probe of photogenerated, charge-*separated* species[11] in the study of the factors controlling electron-transfer rates in such systems.

Acknowledgment. We thank the Science and Engineering Research Council for equipment grants and a postdoctoral research assistantship (to J.N.B.) and for enabling access to the Laser Support Facility. The assistance of the staff of the Facility in setting up the pulsed laser experiments is also gratefully acknowledged. S.E.J.B. thanks the Department of Education (N. Ireland) for a postgraduate studentship and the Queen's University of Belfast for the award of an Andrews Studentship.

---

(9) This is due to some decomposition of the complex by the 360-nm laser pulse, necessitating frequent replenishment of the limited supply of sample available and therefore severely curtailing the number of spectral scans that could be accumulated on the diode array detector.

(10) Angel, S. M.; DeArmond, M. K.; Donohoe, R. J.; Wertz, D. W. *J. Phys. Chem.* **1985**, *89*, 282–285.

(11) Schanze, K. S.; Meyer, T. J. *Inorg. Chem.* **1985**, *24*, 2121–2123.

Department of Chemistry — **John J. McGarvey***
Queen's University of Belfast — **Steven E. J. Bell**
Belfast BT9 5AG, Northern Ireland — **Joseph N. Bechara**

Received June 2, 1986

Correlation between ^{119}Sn Isomer Shifts and Quadrupole Coupling Constants for Dimethyltin(IV) Salts of Strong Protonic Acids and Superacids

Sir:

For a series of dimethyltin(IV) derivatives of very strong protonic acids and superacids, a linear correlation between the ^{119}Sn isomer shift δ (relative to $\mathrm{SnO_2}$) and the quadrupole coupling constant ΔE_Q is noted. The resulting order, apparent from a δ vs. ΔE_Q plot, allows an estimation of relative basicity in the solid state for the corresponding acid and superacid anions present in these $\mathrm{(CH_3)_2Sn}$ derivatives. The purpose of this communication is (a) to identify the structural and spectroscopic features of dimethyltin(IV) salts, allowing a correlation, (b) to provide a rationale for such a correlation between δ and ΔE_Q, and (c) to suggest the use of the $\mathrm{(CH_3)_2Sn}$ group as an electronic probe in the estimation of anion basicities, which may hopefully also be applicable to strongly acidic and superacidic systems.

Table I. ^{119}Sn Mössbauer Data of Dimethyltin(IV) Derivatives of Strong Protonic Acids and Superacids at 77 K

no.[d]	compd	ΔE_Q,[a] mm $\mathrm{s^{-1}}$	δ,[a,b] mm $\mathrm{s^{-1}}$	ref
1	$\mathrm{(CH_3)_2SnF_2}$	4.52	1.23	1
2	$\mathrm{Li_2[(CH_3)_2SnF_4]}$	4.60	1.31	*c*
3	$\mathrm{(CH_3)_2Sn(SO_3\text{-}}p\mathrm{\text{-}CH_3C_6H_4)_2}$	4.85	1.51	5
	$\mathrm{(CH_3)_2Sn(SO_3C_2H_5)_2}$	4.91	1.55	5
4	$\mathrm{(CH_3)_2Sn(SO_3CH_3)_2}$	5.05	1.52	5
5	$\mathrm{(CH_3)_2Sn(PO_2F_2)_2}$	5.13	1.53	4
6	$\mathrm{(CH_3)_2Sn(SO_3Cl)_2}$	5.20	1.75	5
7	$\mathrm{(CH_3)_2Sn(TaF_6)_2}$	5.23	1.69	11
	$\mathrm{Ba[(CH_3)_2Sn(SO_3F)_4]}$	5.37	1.76	10
8	$\mathrm{Cs_2[(CH_3)_2Sn(SO_3CF_3)_4]}$	5.39	1.74	9
	$\mathrm{Cs[(CH_3)_2Sn(SO_3F)_3]}$	5.39	1.80	10
	$\mathrm{Li_2[(CH_3)_2Sn(SO_3F)_4]}$	5.42	1.77	10
9	$\mathrm{Cs_2[(CH_3)_2Sn(SO_3F)_4]}$	5.50	1.83	9
10	$\mathrm{(CH_3)_2Sn(NbF_6)_2}$	5.51	1.77	11
	$\mathrm{(CH_3)_2Sn(SO_3CF_3)_2}$	5.51	1.79	5
11	$\mathrm{(CH_3)_2Sn(SO_3F)_2}$	5.55	1.80	5
12	$\mathrm{(CH_3)_2Sn[Pt(SO_3F)_6]}$	5.67	1.95	9
13	$\mathrm{[(CH_3)_2SnSO_3F]_2[Pt(SO_3F)_6]}$	5.70	1.96	9
14	$\mathrm{(CH_3)_2Sn(Sb_2F_{11})_2}$	6.01	2.08	11
	$\mathrm{(CH_3)_2Sn(SbF_6)_2}$	6.04	2.04	11

[a] Confidence limit ±0.03 mm $\mathrm{s^{-1}}$. [b] Relative to $\mathrm{SnO_2}$ at 77 K. [c] Karunanithy, S.; Aubke, F.; Sams, J. R., to be submitted for publication. [d] Numbers in column 1, refer to data and numbers used in Figure 1.

Solvolysis of either $\mathrm{(CH_3)_4Sn}$, $\mathrm{(CH_3)_3SnCl}$, or $\mathrm{(CH_3)_2SnCl_2}$ in strong protonic acids such as HF, $\mathrm{HPO_2F_2}$, or the sulfonic acids $\mathrm{HSO_3X}$ with X = F, Cl, $\mathrm{CF_3}$, p-$\mathrm{CH_3C_6H_4}$, $\mathrm{CH_3}$, or $\mathrm{C_2H_5}$ is a convenient route to dimethyltin(IV) derivatives of these acids.[1–6] Structures reported for two of the resulting compounds, $\mathrm{(CH_3)_2SnF_2}$[7] and $\mathrm{(CH_3)_2Sn(SO_3F)_2}$,[8] reveal essentially linear C–Sn–C groups with octahedral coordination for tin achieved by weakly coordinated, symmetrically bridging bidentate F or $\mathrm{SO_3F}$ anions. A similar geometry for tin in all dimethyltin(IV) salts of these strong acids is indicated by their ^{119}Sn Mössbauer spectra. Most evident here are the unusually large quadrupole coupling constants, which range from 4.50 to 5.50 mm $\mathrm{s^{-1}}$ and rank among the highest so far reported for tin. Some novel derivatives of these dimethyltin(IV) salts have very recently been synthesized by us[9–11] and their ^{119}Sn Mössbauer spectra exhibit similar, high quadrupole coupling constants. These include anionic derivatives of the types $\mathrm{[(CH_3)_2Sn(SO_3F)_3]^-}$ and $\mathrm{[(CH_3)_2Sn(SO_3X)_4]^{2-}}$ with X = F or $\mathrm{CF_3}$, which have ΔE_Q values of ~5.4–5.5 mm $\mathrm{s^{-1}}$,[9,10] while cationic derivatives with either $\mathrm{[(CH_3)_2Sn(SO_3F)]^+}$ or $\mathrm{(CH_3)_2Sn^{2+}}$, stabilized by anions like $\mathrm{[M(SO_3F)_6]^{2-}}$, with M = Sn or Pt,[9] or by $\mathrm{SnF_6^{2-}}$,[11] show ΔE_Q values between 5.50 and 5.70 mm $\mathrm{s^{-1}}$. Finally, for dimethyltin(IV) salts with either $\mathrm{Sb_2F_{11}^-}$ or $\mathrm{SbF_6^-}$ as counteranions, exceptionally high quadrupole coupling constants of ~6.0 mm $\mathrm{s^{-1}}$ are observed.[11] These cationic salts and their $\mathrm{TaF_6^-}$ and $\mathrm{NbF_6^-}$ analogues may be viewed as derived from superacids such as $\mathrm{HF\text{-}SbF_5}$ or $\mathrm{HSO_3F\text{-}Pt(SO_3F)_4}$.[12]

The ^{119}Sn Mössbauer parameters for all these $\mathrm{(CH_3)_2Sn}$ derivatives are listed in Table I in order of increasing ΔE_Q values. A few additional examples in this series, those with two different tin environments, as e.g. $\mathrm{(CH_3)_2Sn[SnF_6]}$, are omitted because

---

(1) Levchuk, L. E.; Sams, J. R.; Aubke, F. *Inorg. Chem.* **1972**, *11*, 43.

(2) Yeats, P. A.; Ford, B. F. E.; Sams, J. R.; Aubke, F. *J. Chem. Soc., Chem. Commun.* **1969**, 151.

(3) Schmeisser, M.; Sartori, P.; Lippsmeier, B. *Chem. Ber.* **1970**, *103*, 868.

(4) Tan, T. H.; Dalziel, J. R.; Yeats, P. A.; Sams, J. R.; Thompson, R. C.; Aubke, F. *Can. J. Chem.* **1972**, *50*, 1843.

(5) Yeats, P. A.; Sams, J. R.; Aubke, F. *Inorg. Chem.* **1972**, *11*, 2634.

(6) Birchall, T.; Chan, P. K. H.; Pereira, A. R. *J. Chem. Soc., Dalton Trans.* **1974**, 2157.

(7) Schlemper, E. O.; Hamilton, W. C. *Inorg. Chem.* **1966**, *5*, 995.

(8) Allen, F. H.; Lerbscher, J. A.; Trotter, J. *J. Chem. Soc. A* **1971**, 2507.

(9) Mallela, S. P.; Tomic, S. T.; Lee, K.; Sams, J. R.; Aubke, F. *Inorg. Chem.* **1986**, *25*, 2939.

(10) Mallela, S. P.; Yap, S.; Sams, J. R.; Aubke, F. *Inorg. Chem.*, in press.

(11) Mallela, S. P.; Yap, S.; Sams, J. R.; Aubke, F. *Rev. Chim. Miner.*, in press.

(12) Mallela, S. P.; Lee, K. C.; Aubke, F. *Inorg. Chem.* **1984**, *23*, 653.

0020-1669/86/1325-4327$01.50/0

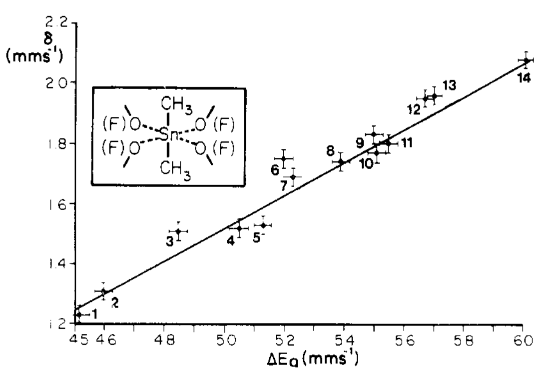

Figure 1. Correlation of ^{119}Sn isomer shift (δ) and the quadrupole splitting (ΔE_Q) for dimethyltin(IV) salts of strong protonic acids and superacids.

here partly overlapping absorption lines cause some uncertainty in both the δ and ΔE_Q values.

Quadrupole coupling constants for all the compounds listed are well in excess of 4.12 mm s^{-1}, the value previously suggested as the maximum ΔE_Q value for octahedral $(CH_3)_2Sn$ compounds with linear C–Sn–C groups.[13] More intriguingly, there is a gradual concomitant increase in isomer shift δ with increasing quadrupole coupling constant found for the dimethyltin(IV) salts listed in Table I, and a plot of ΔE_Q vs. δ (relative to SnO_2) for representative dimethyltin(IV) compounds gives the reasonably good straight line shown in Figure 1, which also shows a picture of the suggested geometrical arrangement around tin. This linear correlation, as well as the magnitude of δ and more so of ΔE_Q, sets the dimethyltin(IV) salts discussed here clearly apart from the dimethyltin(IV) complexes that had formed the experimental bases for the application of the point-charge model to dimethyltin(IV) compounds,[13] and a different electronic structure for the $(CH_3)_2Sn$ salts is indicated.

The two reported structures,[7,8] evidence from Raman and IR spectra,[2,4,5,9-11] and the large ΔE_Q values all leave little doubt regarding the geometrical structure of the dimethyltin(IV) salts: a linear or nearly linear C–Sn–C group with octahedral coordination completed by either four oxygen or four fluorine atoms belonging to the weakly basic anions. Axial geometry implies that V_{zz}, the principal component of the electric field gradient (efg) tensor along the z axis, is large and negative and η, the asymmetry parameter, is either zero or negligible. This in turn implies large positive values for the quadrupole coupling constant since for ^{119}tin ΔE_Q and V_{zz} carry opposite signs.

Clark et al.[14] have shown that the efg at tin arises almost entirely from unequal populations of the Sn 5p orbitals, and that contributions from 5d orbital occupancy are negligible. The contribution to V_{zz} from an electron in a p_z orbital is $-(^4/_5)e\langle r^{-3}\rangle_p$, whereas that from an electron in either a p_x or p_y orbital is $+(^2/_5)e\langle r^{-3}\rangle_p$, where e denotes the protonic charge, and $\langle r^{-3}\rangle_p$ denotes radial averages for p orbitals. Thus, the large negative V_{zz} values in the present compounds clearly indicate a strong imbalance in p-orbital charge densities at tin, with most of the p-electron density localized in the axial direction, i.e. in the p_z orbital.

On the other hand, the isomer shift is proportional to the 5s-electron density at the nucleus, and the very high δ values observed indicate some of the highest s-electron densities ever found in tin(IV) compounds.

In the limiting case, the "pure" $(CH_3)_2Sn^{2+}$ cation, covalent bonding to carbon would involve $5sp_z$ hybrid orbitals and a valence state of $5s^15p_z^1$ on tin. This limiting case appears to be approximated closely by $(CH_3)_2Sn(SbF_6)_2$ and $(CH_3)_2Sn(Sb_2F_{11})_2$ where observed isomer shifts equal, within limits of error, the value for α-tin, which has an identical $5s^1$ electron population in its valence state and is generally regarded as marking the dividing line between Sn(II) and Sn(IV).[15,16] Consistent with this view, ΔE_Q values observed for these two compounds are, with 6.0 mm s^{-1}, approximately 0.5 mm s^{-1} greater than the largest value previously reported.[2,5]

Increasing nucleophilicity of the anionic group(s) around the $(CH_3)_2Sn^{2+}$ cation, resulting in enhanced cation–anion interaction via the Sn p_x and p_y orbitals, would decrease both ΔE_Q and δ, by decreased p-orbital charge imbalance and increased s-electron screening, respectively. The observation of a linear relation between these two parameters suggests that the dominant effect of the increased anion nucleophilicity is simply to partially populate the Sn p_x and p_y orbitals, which does not result in significant rehybridization of the tin bonding orbitals.

Consistent with this view is the observation that anionic complexes of the type $[(CH_3)_2SnX_4]^{2-}$, with X = F, SO_3F or SO_3CF_3 coordinated in a monodentate mode, exhibit Mössbauer parameters that are approximately identical within error limits to those found for the corresponding neutral $(CH_3)_2SnX_2$ species with bidentate coordination of X. The implication is that anion nucleophilicity is controlling the electronic structure of tin, independent of anion coordination or net negative charge of the resulting complex anions.

With most of the anions discussed here, derived from strong protonic acids or superacids, an additional conclusion is possible. The ability of these systems to protonate substrates and/or to stabilize highly electrophilic cations is strongly influenced by the nucleophilicity of these anions, as is evident from simple proton-transfer equilibria

$$2HA_{solv} \rightleftarrows H_2A^+_{solv} + A^-_{solv} \qquad (1)$$

where A$^-$ is an acid anion, or in the case of superacids

$$2HA_{solv} + Y_{solv} \rightleftarrows H_2A^+_{solv} + AY^-_{solv} \qquad (2)$$

where Y is a Lewis acid and AY$^-$ a superacid anion.

While it has been possible to measure or estimate, in most cases, the acidity of these systems, with the Hammett H_0 scale being the most generally used method of ordering,[17] or to derive from the experimental data an order of Lewis acidity for Y,[18] it has not been possible to estimate the nucleophilicity of these extremely weakly basic anions A$^-$ or AY$^-$, respectively. The use of ^{119}Sn Mössbauer spectroscopy, with the dimethyltin(IV) cation acting as an electronic structure probe, provides an order of solid-state basicities, which may, however, be slightly different from solution acidity data,[18] as illustrated by the ranking of TaF_6^- below NbF_6^-,[11] with NbF_5 generally viewed as a weaker Lewis acid than TaF_5.[18] Nevertheless, a useful order emerges, as is apparent from Figure 1, with SbF_6^- or $Sb_2F_{11}^-$ as the least basic anions, just as SbF_5 is viewed as the strongest Lewis acid. Furthermore, it becomes possible to include in this comparison anions formed either by protonic acids like HSO_3CF_3, which are not derived from Lewis acids, or by superacid systems like HSO_3F–$Pt(SO_3F)_4$, where the Lewis acidity of $Pt(SO_3F)_4$ has not been estimated.

It is anticipated that this correlation can be extended to other dimethyltin(IV)–oxyacid salts with linear C–Sn–C groups. We have presently used data from our laboratories exclusively, and attempts to extend this correlation to other dimethyltin(IV) salts, in particular those with fluoro anions, are currently being undertaken.

It remains to mention that a similar δ vs. ΔE_Q correlation is reported for a more diverse group of pentacoordinated trimethyltin(IV) complexes.[19] In addition, the use of ρ, the ratio of the quadrupole splitting to isomer shift (relative to SnO_2), first proposed by Herber et al.[20] for organotins, has generally been

---

(13) Sham, T. K.; Bancroft, G. M. *Inorg. Chem.* **1975**, *14*, 2281.

(14) Clark, M. G.; Maddock, A. G.; Platt, R. H. *J. Chem. Soc., Dalton Trans.* **1972**, 281.

(15) Donaldson, J. D.; Tricker, M. J. *Spec. Period. Rep.: Spectrosc. Prop. Inorg. Organomet. Compd.* **1979**, 381.

(16) Zuckerman, J. J. In *Chemical Mössbauer Spectroscopy*; Herber, R. H., Ed.; Plenum: New York, 1984; p 267.

(17) Olah, G. A.; Prakash, G. K. S.; Sommer, J. *Superacids*; Wiley: New York, 1985; and references therein.

(18) Fabre, P. L.; Devynck, J.; Termillon, B. *Chem. Rev.* **1982**, *82*, 591 and references therein.

(19) Ruddick, J. N. R.; Sams, J. R. *Chem. Phys. Lett.* **1974**, *28*, 548.

(20) Herber, R. H.; Stöckler, H. A.; Reichle, W. T. *J. Chem. Phys.* **1965**, *42*, 2447.

extremely useful in identifying associated structures.[16] The correlation described here is more limited in scope and is intended to rationalize some of the more unusual ^{119}Sn Mössbauer data reported over the years for dimethyltin(IV) derivatives. However, the suggested use of the dimethyltin(IV) group as an electronic structure probe and the order of anion basicities, evident from the δ vs. ΔE_Q plot, go beyond the use of ^{119}Sn Mössbauer spectra as a molecular structure probe for organotin(IV) compounds.[20]

Acknowledgment. Our research is supported by the Natural Sciences and Engineering Research Council of Canada.

---

(21) Present address: Department of Chemistry, University of Idaho, Moscow, ID 83843.

Department of Chemistry
The University of British Columbia
Vancouver, BC, V6T 1Y6 Canada

S. P. Mallela[21]
S. Yap
J. R. Sams
F. Aubke*

Received June 17, 1986

Synthesis and Crystal Structure Determination of a Propylene Glycol Bridged Molybdenum(VI) Peroxo Dimer, $[MoO(O_2)(C_3H_6O_2)(CH_3OH)]_2·2CH_3OH$

Sir:

Molybdenum(VI) peroxo complexes are stoichiometric reagents[1] and catalysts[2] for olefin epoxidation. Single-crystal X-ray diffraction studies have shown that the organic ligands contained in this class of compound can be covalently bonded[3–10] or loosely coordinated[11–14] to the Mo(VI) center. Despite the large family of polynuclear peroxomolybdates reported in the literature,[15] all these ligand-stabilized peroxo complexes except the hydroperoxide-bridged $[Mo_2O_2(O_2)_4(OOH)_2]^{2-}$ anion[4] and the tartrate-bridged $[Mo_2O_2(O_2)_4(C_4H_2O_6)]^{4-}$ anion[10] are monomeric. This paper reports the synthesis and solid-state structure of $[MoO(O_2)(C_3H_6O_2)(CH_3OH)]_2·2CH_3OH$ (**1**), the first structurally characterized nonionic polynuclear Mo(VI) peroxo complex with a covalently bonded diolate ligand. The unique structural features of this compound provide insights in the design of more effective early-transition-metal peroxo complexes for asymmetric epoxidation of olefinic substrates.

In the synthesis of **1**, the dioxomolybdenum(VI) propylene glycolate complex $MoO_2(C_3H_7O_2)_2$[16] was first prepared from the ligand exchange reaction of $MoO_2(acac)_2$ with 1,2-propanediol in dichloromethane. Dissolution of this propylene glycolate complex in a *tert*-butyl alcohol solution of anhydrous *tert*-butyl hydroperoxide at 70 °C followed by slow diffusion of anhydrous methanol under argon over a 2-day period gave bright yellow crystals of **1** suitable for single-crystal X-ray diffraction study.[17] Alternatively, **1** can be prepared by reacting peroxomolybdic acid[18] with 1,2-propanediol in anhydrous methanol at 25 °C under an inert atmosphere.

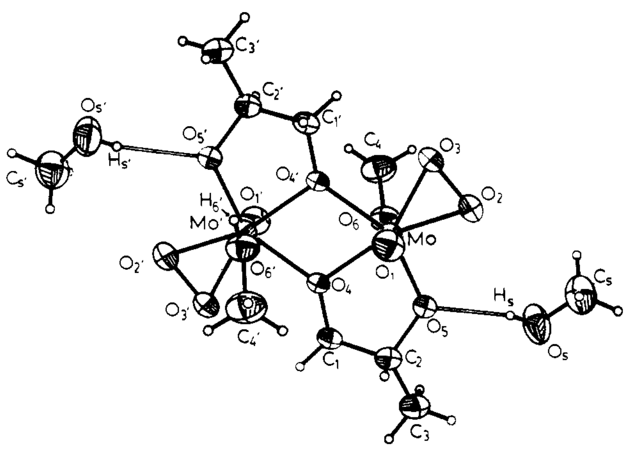

Figure 1. ORTEP drawing of **1** with molybdenum, oxygen, and carbon atoms represented by thermal vibration ellipsoids drawn to encompass 50% of their electron density. Hydrogen atoms are represented by arbitrarily small spheres. Hydrogen atom H_6 is hidden from view in this orientation. Atoms labeled with a prime (′) are related to those without primes by the crystallographic inversion center at $^1/_2$, 0, $^1/_2$. Selected bond lengths and angles: $Mo–O_1$ = 1.665 (2) Å, $Mo–O_2$ = 1.925 (2) Å, $Mo–O_3$ = 1.916 (2) Å, $Mo–O_4$ = 2.070 (2) Å, $Mo–O_4'$ = 2.061 (2) Å, $Mo–O_5$ = 1.944 (2) Å, $Mo–O_6$ = 2.300 (2) Å, $O_2–O_3$ = 1.451 (3) Å, $H_6 \cdots O_S$ = 1.88 (4) Å, $H_S \cdots O_5$ = 2.11 (4) Å, $O_4–Mo–O_5$ = 77.4 (1)°, $O_4–Mo–O_4'$ = 69.5 (1)°.

Compound **1** forms monoclinic crystals: space group $P2_1/n$ (alternate setting of $P2_1/c$-C_{2h}^5 (No. 14)); a = 7.878 (2) Å, b = 9.307 (3) Å, c = 14.194 (4) Å, β = 99.44 (2)°; Z = 2 dimer units; d_{calcd} = 1.825 g cm^{-3}. X-ray diffraction data at 20 °C were collected on a computer-controlled four-circle Nicolet autodiffractometer using graphite-monochromated Mo K$\bar{\alpha}$ radiation. The structure was solved by heavy-atom Patterson techniques. Of 2353 independent reflections collected to 2θ(Mo K$\bar{\alpha}$) = 55°, 1815 having $I > 3\sigma(I)$ were used in the final least-squares refinement cycle to give R_F and R_w values of 2.4% and 2.6%, respectively.

The title compound depicted in Figure 1 exhibits several distinctive structural features. The two halves of **1** are related by a crystallographic inversion center and bridged by the diolate oxygens of a pair of 1,2-propanediol enantiomers. The binding mode of the glycolate ligand is similar to that of the tartramide and tartrate ester ligands found in the two dinuclear titanium catalysts[19] used for asymmetric epoxidation of allylic alcohols. The planar Mo_2O_2 core is almost a symmetric rhombus with $Mo–O_4$ and $Mo–O_4'$ bond distances of 2.070 (2) and 2.061 (2) Å, respectively; the internuclear Mo---Mo′ separation is 3.395 (1) Å. The peroxy and diolate oxygens form the equatorial plane of a distorted pentagonal bipyramid with a terminal oxygen and the methanol oxygen at the apices. The Mo—peroxo distances, the Mo═O distance, and the O—O distance in the peroxo group are all within the range of distances previously observed for this class of peroxo complexes. The hydroxy proton on each of the coordinated methanol molecules (H_6 or H_6') is hydrogen-bonded to a hydroxy oxygen (O_S or O_S') of a symmetry-related methanol

---

(1) Mimoun, H.; Seree de Roch, I.; Sajus, L. *Tetrahedron* **1970**, *26*, 37.
(2) Westland, A. D.; Haque, F.; Bouchard, J. M. *Inorg. Chem.* **1980**, *19*, 2255.
(3) Stomberg, R. *Acta Chem. Scand.* **1970**, *24*, 2032.
(4) LeCarpentier, J. M.; Mitschler, A.; Weiss, R. *Acta Crystallogr., Sect. B: Struct. Crystallogr. Cryst. Chem.* **1972**, *B28*, 1288.
(5) Edwards, A. J.; Slim, D. R.; Guerchais, J. E.; Kergoat, R. *J. Chem. Soc., Dalton Trans.* **1977**, 1966.
(6) Jacobson, S. E.; Tang, R.; Mares, F. *Inorg. Chem.* **1978**, *17*, 3055.
(7) Chaumette, P.; Mimoun, H.; Saussine, L.; Fischer, J.; Mitschler, A. *J. Organomet. Chem.* **1983**, *250*, 291.
(8) Flanagan, J.; Griffith, W. P.; Skapski, A. C.; Wiggins, R. W. *Inorg. Chim. Acta* **1985**, *96*, L23.
(9) Djordjevic, C.; Covert, K. J.; Sinn, E. *Inorg. Chim. Acta* **1985**, *101*, L37.
(10) Dengel, A. C.; Griffith, W. P.; Powell, R. D.; Skapski, A. C. *J. Chem. Soc., Chem. Commun.* **1986**, 555.
(11) LeCarpentier, J. M.; Schlupp, R.; Weiss, R. *Acta Crystallogr., Sect. B: Struct. Crystallogr. Cryst. Chem.* **1972**, *B28*, 1278.
(12) Winter, W.; Mark, C.; Schurig, V. *Inorg. Chem.* **1980**, *19*, 2045.
(13) Schlemper, E. O.; Schrauzer, G. N.; Hughes, L. A. *Polyhedron* **1984**, *3*, 377.
(14) Djordjevic, C.; Vuletic, N.; Sinn, E. *Inorg. Chim. Acta* **1985**, *104*, L7.
(15) For a listing of the known peroxopolymolybdates, see: Persdotter, I.; Trysberg, L.; Stomberg, R. *Acta Chem. Scand., Sect. A* **1986**, *A40*, 83 and references cited therein.
(16) Sheldon, R. A. *Recl. Trav. Chim.* **1973**, *92*, 367.
(17) Compound **1** is moisture-sensitive and eventually decomposes to molybdenum blue on sitting at room temperature; hence, all manipulations were carried out under an atmosphere of dry argon. A satisfactorily grown crystal with dimensions of 0.30 × 0.40 × 0.75 mm was immediately sealed with the solvent inside a thin-walled capillary for X-ray data collection. The structure determination was carried out by Dr. C. S. Day of Crystalytics, Lincoln, NE 68501.
(18) Kaloustian, J.; Lena, L.; Metzger, J. *Tetrahedron Lett.* **1975**, 559.
(19) Williams, I. D.; Pedersen, S. F.; Sharpless, K. B.; Lippard, S. J. *J. Am. Chem. Soc.* **1984**, *106*, 6430.

0020-1669/86/1325-4329$01.50/0